MEMOIRS OF THE FACULTY OF ENGINEERING
FUKUI UNIVERSITY
VOL.26 No.1 1978

Relaxed Excitonic States in Cadmium Halide Crystals (I)
—— $CdBr_2$ and $CdBr_2$:I ——

Hideyuki NAKAGAWA*, Keiji HAYASHI*, Hiroaki MATSUMOTO*

(Received Dec. 15, 1977)

Experimental studies on luminescence have been made in $CdBr_2$ and $CdBr_2$:I to obtain informations about the relaxed excitonic state in cadmium halide crystals. The intensity, life-time and linear polarization of the luminescence have been measured as a function of temperature in the region above 10 K. The UV-emission observed at 3.30 eV in $CdBr_2$ and at 3.35 eV in $CdBr_2$:I is dominant below 60 K and decays radiatively with relatively short life-time, 0.6 μs in $CdBr_2$ and 0.3 μs in $CdBr_2$:I, which is independent of temperature below 50 K. The Y-emission observed at 2.15 eV in $CdBr_2$ is dominant above 60 K and decays radiatively with a relatively long life-time which depend on temperature with a complex fashion. The G-emission observed at 2.52 eV in $CdBr_2$:I is dominant above 60 K, with radiative life-time of 3 μs which is independent of temperature from 70 K to 160 K. The UV-emission is highly polarized perpendicularly to the crystal *c*-axis at LHeT and the values of the degree of polarization, *P*, decrease rapidly with raising temperature, from 0.3 at LHeT to 0.05 at LNT in $CdBr_2$ and from 0.5 at LHeT to 0.1 at LNT in $CdBr_2$:I, respectively. The values of *P* of the Y- and G-emission are approximately constant independent of temperature above 70 K. Polarization correlation between the exciting and emitted light was observed for the UV-emission of $CdBr_2$ at LHeT only when the excitation was made in the region of the 4.95 eV absorption band in $CdBr_2$. The experimental results obtained in the present study are well explained by using, as a model for the relaxed excitonic states in $CdBr_2$, the excited states of the complex molecular ion consisting of a central cadmium and six neiboring bromine ions, $[Cd^{2+}Br_6^-]^{4-}$. In particular, polarization characteristics of the UV-emission is satisfactorily ex-

*Dept. of Electronics.

plained with this model by introducing the spin-orbit and electron-hole exchange interactions in addition to the D_{3d} crystal field.

1. Introduction

Layered matarials, with their strong anisotropic properties along different crystallographic directions, have attracted the attension of many physicists in recent years[1]. Cadmium bromide is one of ionic crystals of such a layered structure[2], the crystal structure of which is shown in Fig. 1. This is a trigonal one with one molecule in a unit cell and belongs to the $CdCl_2$-type with the space group of D_{3d}^5. The crystal is made up of layers of bromine ions (open circles) which are nearly cubic close-packed, with cadmium ions (solid circles) sandwiched between alternate bromine layers. The crystal *c*-axis is perpendicular to these layers. As shown in the figure, each cadmium ion is located at the center of an octahedron consisting of six bromine ions which is compressed along the *c*-axis. The point symmetry of the complex molecular ion consisting of a central cadmium and six neighboring bromine ions, $[Cd^{2+}Br_6^-]^{4-}$, is D_{3d} with one three-fold axis, the crystal *c*-axis, and three two-fold axes as shown also in the figure.

It is well known that cadmium halide crystals show strong luminescence at low temperature when excited with ultra-violet light in the fundamental absorption region[3,4]. These luminescence can be associated with the radiative decay of the relaxed excitonic states (refered as the RES in the following) and are characterized by the constituent halogen ions. In the previous reports, which are concerned with

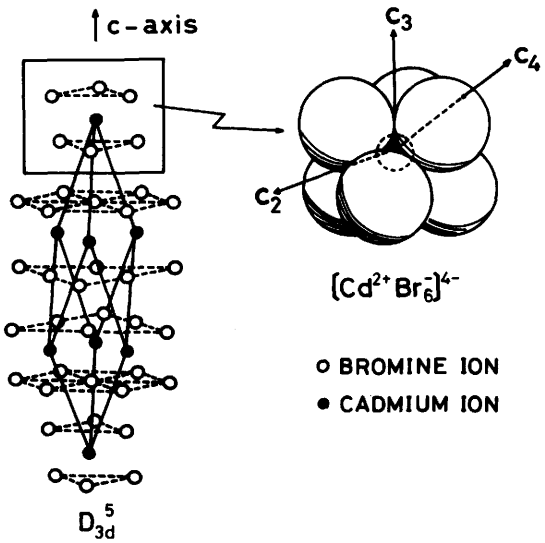

Fig. 1 Crystal structure of $CdBr_2$. The crystal is made up of layers of bromine ions which are nearly cubic close-packed, with cadmium ions sandwiched between alternate bromine layers. The crystal *c*-axis is perpendicular to the layers. Each cadmium ion is located at the center of an octahedron consisting of six bromine ions which is compressed along the *c*-axis. The unit cell is outlined with solid lines.

optical absorption and luminescence in the mixed crystals of $CdCl_2$-$CdBr_2$[5,6] or $CdCl_2$-$CdBr_2$:I[7], it has been proposed that the RES in cadmium halide crystals can be approximated by the excited states of the $[Cd^{2+}X_6^-]^{4-}$-complex molecular ions (X^-=Cl^-or Br^-), just mentioned above.

In this paper will be presented the experimental results on luminescence in $CdBr_2$ and $CdBr_2$:I. The luminescence intensity, life-time and linear polarization have been measured as a function of temperature in the region above 10 K. Some discussion will be made on the relaxed excitonic states in these systems by using the excited states of the $[Cd^{2+}Br_6^-]^{4-}$-complex molecular ions, the symmetry of which is D_{3d}. The spin-orbit and exchange interactions will be also taken account of to examine the polarization characteristics of luminescence.

2. Experimentals

2.1. Samples

Single crystals of $CdBr_2$ and $CdBr_2$:I were grown from the melt using Stockbarger techniques. Special reagent-grade powder of hydrated salts was dehydrated in vacume and sealed into quartz ampoules. For the growing of $CdBr_2$:I crystals, the CdI_2 powder of about 1 mol percent were mixed with the $CdBr_2$ powder. The concentration check for the crystals used in each measurement was not performed in the present work.

Specimens were mounted on the sample holder of a metal cryostat and were cooled by conduction. Temperature of the specimen was controlled by a electric heater attached to the sample holder and was measured with a calibrated Au:Co-chromel thermo- couple.

For the polarization measurements were prepared the specimens of

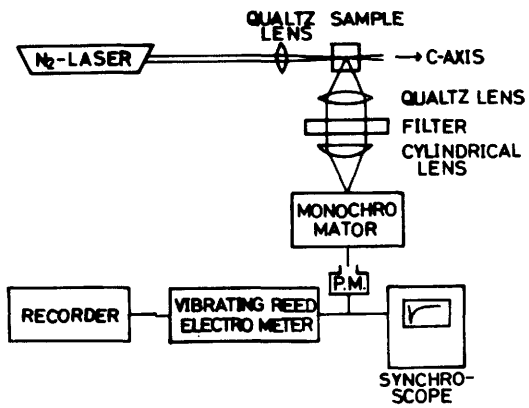

Fig. 2 Schematic representation of the optical equipment for the measurements of luminescence life-time. The light pulses from the N_2-laser were focused on the crystal along the crystal *c*-axis. Out-put signals from the photomultiplier were displayed on a screen of a synchroscope. The spectral distribution of luminescence was also measured by using a vibrating reed electrometer and a recorder. A thick filter was used for the sake of cutting off intense laser light scattered in the direction of measurements.

parallel piped shape. The crystal ingot was first cleaved perpendicularly to the crystal *c*-axis and surfaces parallel to the axis were cut and polished with some cotton in ethyl-alcohol.

2.2. Measurements of life-time

Experimental set-up for the measurements of life-time is shown in Fig. 2. Excitation was made by two photon absorption processes with a 3371 A light pulse of short duration (10 ns) from a nitrogen gas laser. The light pulse was incident on the sample along the *c*-axis, giving rise to the emission of luminescent light. The emitted light was monitored perpendicular to the direction of the incident radiation by a HTV-931A photomultiplier through an adequate filter and an analyzing monochromator to select each emission band of the crystal phosphor. The output signals were displayed on the screen of IWATSU SS112 100MHz synchroscope and were photographed. Obtained decay curves were decomposed to two or three exponential curves in some cases. This was made by the graphical method using semilogarithmic section papers.

2.3. Measurements of polarization

Fig. 3 shows experimental set-up for the measurements of the polarization characteristics of luminescence. The exciting light was incident along the crystal *c*-axis and, therefore, its electric vector was in the plane perpendicular to the axis. Luminescnce intensities were detected in the direction perpendicular to this. Only the light flux close to the optical axis was selected by two or three diaphragms. The polarization direction of luminescence was analyzed by a Frank-

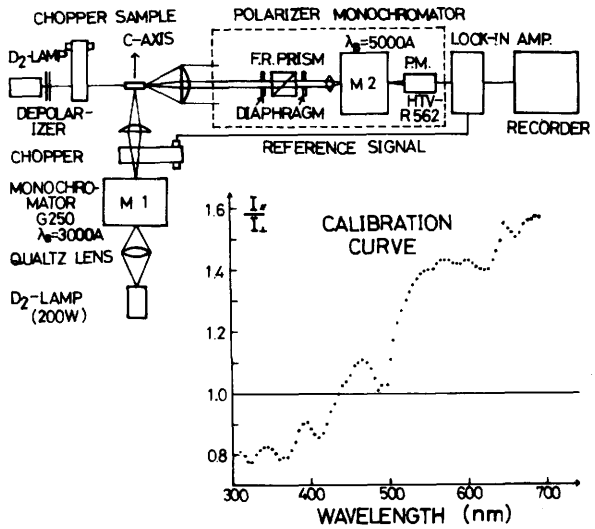

Fig. 3 Experimental set-up for the measurements of the polarization characteristics of luminescence. Nonpolarized incident radiation was led along the crystal *c*-axis and luminescence was detected in the direction perpendicular to this. Two or three diaphragms were used to select only the light flux close to the optical axis. The inset shows the inherent polarization characteristics of the analyzing system, which is enclosed by a dashed line, as a function of wavelength. This calibration curve was obtained by using the depolarized light.

Ritter prism. Analyzed light was led to a NICON G250 grating monochromator, M2, and detected by an end-on type HTV-R562 photomultiplier. The output signals from the photomultiplier were measured by a NF-LI-573 lock-in amplifier and a pen recorder.

The inherent polarization characteristics of the luminescence analyzing system, which is shown in the figure enclosed by a dashed line, were measured by using the depolarized light which was obtained by combining a D_2-lamp of a cylindrical shape with a depolarizer consisting of two sheets of powder paper. It was confirmed experimentally that there occur no changes in the output signals when rotating the D_2-lamp with the depolarizer around the optical axis. The measured results are also shown in the figure by a dotted curve, where $I_{//}$ and $I_{\perp}$ indicate the light intensities polarized along and perpendicularly to the entrance slit direction of the monochromator, M2, respectively, that is $I_{//}$ corresponds to the light polarized perpendicularly to the plane of this figure and $I_{\perp}$ to that parallel to it. It should be noted that the values of the polarization ratio, $r = I_{//}/I_{\perp}$, varies extensively with the wavelength of the light. This curve was used as a calibration curve to correct the measured polarization ratio of luminescence.

In Fig. 4 are shown the excitation system used in the measurements of the polarization correlation between the exciting and the emitted light. Polarized ultra-violet light was selected by using two Wallaston prisms. The system including two Wollaston prisms, a qualtz lens and a D_2-lamp, enclosed by a dashed line in the figure, was set up so as the light spot of the extraordinary ray was fixed on the center of the grating of the monochromator, M1, when the system was rotated as a whole around the entrance optical axis of M1. By masking the front surface of the grating, it was possible for only the extraordinary ray to get through M1. The direction of polarization with respect to that of entrance slit of M1 was able to be set at will by this mechanism. The specimen was set as

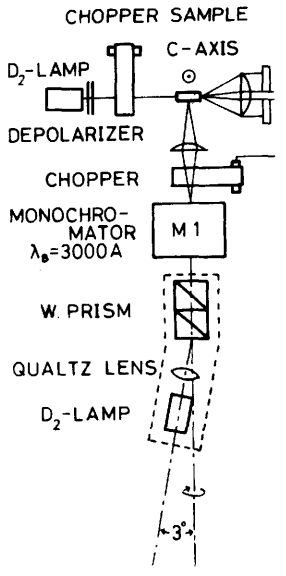

Fig. 4 Polarized light excitation system. The system enclosed by a dashed line was set to be rotated as a whole around the entrance optical axis of M1. Polarized ultra-violet light was selected by using two Wollaston prisms.

shown in the figure, with the crystal c-axis perpendicular to both exciting and emitted light beams.

3. Experimental Results

In Fig. 5 are shown optical absoption spectra of $CdBr_2$ and $CdBr_2$:I observed at liquid nitrogen temperature (LNT). The solid curve in this figure was obtained on a thin film of pure $CdBr_2$. Two pronounced peaks at 5.18 eV and 5.76 eV are believed to constitute a spin-orbit doublet of bromine ions[8]. Another structure appears at about 4.95 eV, which is associated with the crystal field splitting of excitonic states due to the trigonal field, C_{3v}, at the bromine ion sites[9]. A plausible energy diagram of the excitonic states responsible for these absorption structures will be shown later. A broken line shows an absorption spectrum obtained on a single crystal of $CdBr_2$ which contains a small amount of iodine ions (0.1 mol%). Sharp rise of absorption around 4.7 eV is the intrinsic absorption edge of $CdBr_2$. An additional absorption band appears at 4.57 eV by doping iodine ions. This is a localized excitonic absorption band due to doped iodine ions[10] like as those well-known in alkali haides such as in KCl:I[11].

Under excitation with ultra-violet light in the regions of intrinsic or localized excitonic absorption bands, two prominet emission bands were observed as shown in Fig. 6[6,12]. In this figure, solid and dashed curves represent the emission spectra obtained at liquid helium temperature (LHeT) and LNT, respectively. In $CdBr_2$, illumination in the fundamental absorption region gives rise to the emissions at 3.30 and 2.15 eV. These emissions are believed to be intrinsic ones. In $CdBr_2$:I, which contains about one mol percent of iodine ions, the

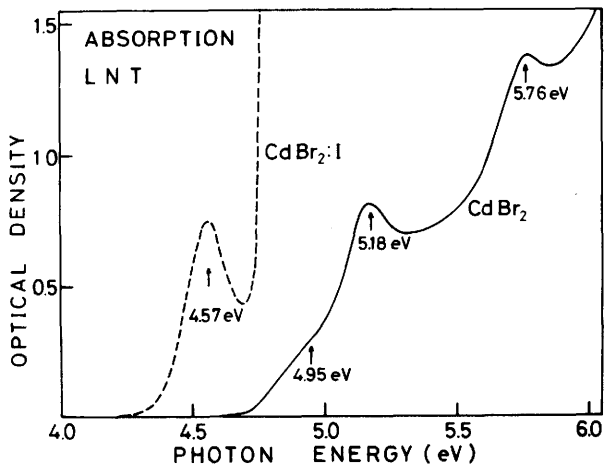

Fig. 5 Optical absorption spectra of $CdBr_2$ and $CdBr_2$:I observed at liquid nitrogen temperature. The solid curve was obtained on a thin film of pure $CdBr_2$. The broken line shows an absorption spectrum obtained on a single crystal of $CdBr_2$ which contains a small amount of iodine ions. Sharp rise of absorption around 4.7 eV is the intrinsic absorption edge of $CdBr_2$.

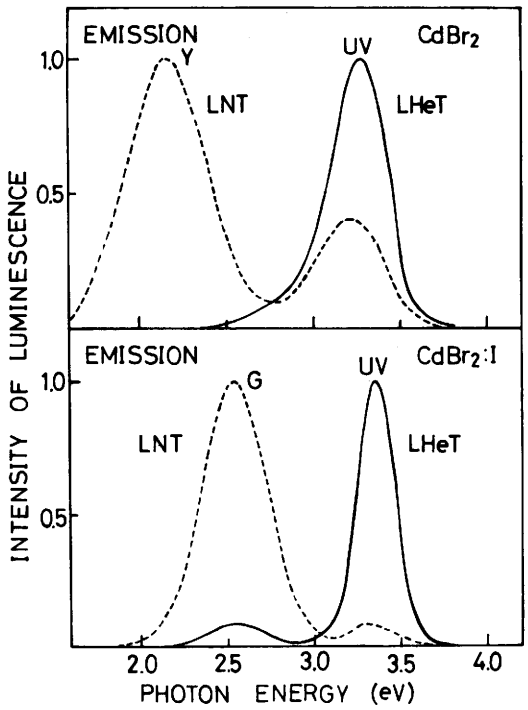

Fig. 6 Emission spectra of $CdBr_2$ and $CdBr_2$:I. Solid and dashed curves represent the emission spectra obtained at LHeT and LNT, respectively. Excitation was made at 5.18 eV in the fundamental absorption region for $CdBr_2$ and at 4.57 eV in the localized excitonic absorption band due to the doped I^--ions for $CdBr_2$:I. Each emission band is named according to their spectral positions. The intensities of luminescence are normalized to unity at the maximum.

emissions at 3.35 and 2.52 eV are observed by the excitation in the localized excitonic absorption band due to iodine ions. In the following, luminescence around 3.30 eV is named the UV-emission, that at 2.15 eV the Y-emission and that at 2.52 eV the G-emission. As perceived in this figure, the UV-emission is dominant at LHeT and the Y- or G-emission become dominant at LNT.

The temperature dependence of the lumnescence intensities and life-times of these emissions are shown in Figs. 7 and 8.

Fig. 7 shows the case of $CdBr_2$. The broken lines, I_{UV} and I_Y, show the temperature dependence of intensities of the UV- and the Y-emissions, respectively. The intensity of the UV-emission, which is dominant at low temperature, decreases around 60 K, and, instead, the Y-emission increases its intensity. This change of intensities with raising temperature is expressed by a thermal activation process of the activation energy ΔE = 0.05 eV. The Y-emission is quenched above 150 K by the nonradiative transition with the activation energy ΔE = 0.21 eV. The total intensities of these emissions are held constant independent of temperature below 150 K. The temperature dependence of the life-times of these emissions is also shown in this figure. The life-time τ is defined in the present paper as the time interval

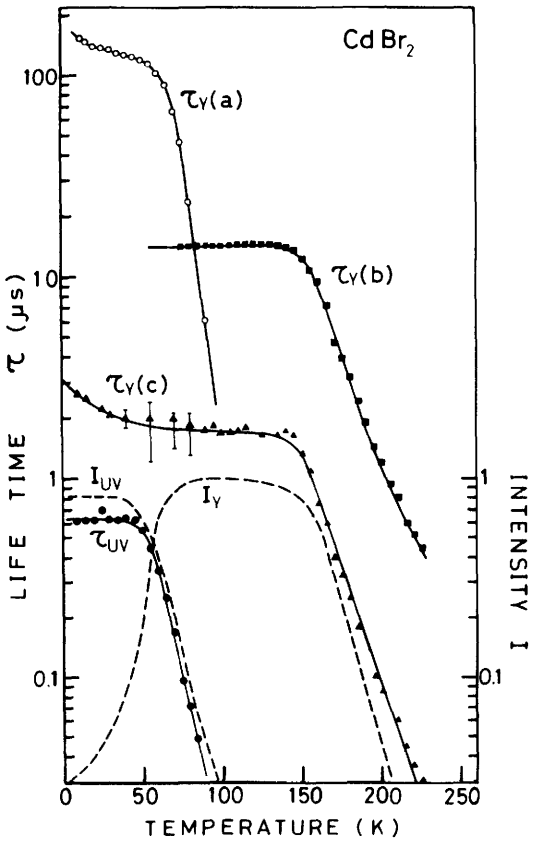

Fig. 7 The temperature dependence of the luminescence intensities and life-times of each emission in $CdBr_2$. The broken lines, I_{UV} and I_Y, show the temperature dependence of intensities of the UV- and the Y-emissions, respectively. The scale of the intensity is indicated on the right side ordinate. τ_{UV} and τ_Y are the life-times of the UV- and the Y-emission, respectively. The decay curves of the Y-emission is composed of three components which are shown by open circles (a), solid squares (b) and solid triangles (c). The life-time τ is defined here as the time interval during which the luminescence intensity reduces to half as much as the initial one.

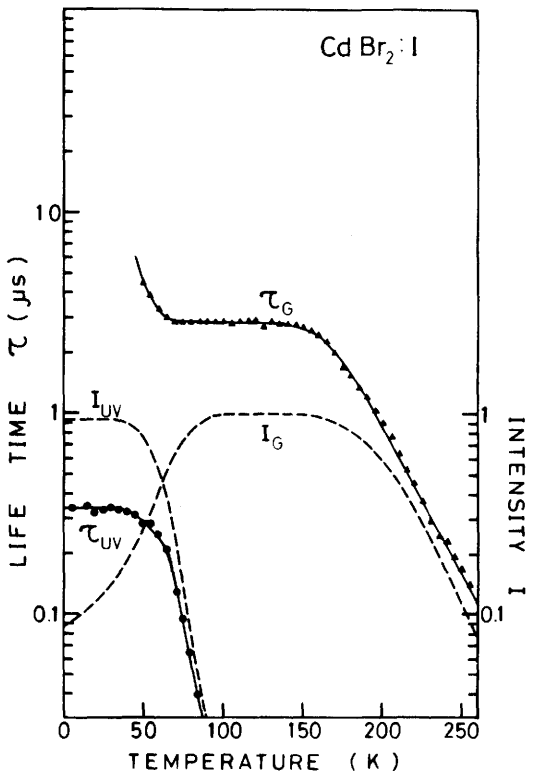

Fig. 8 The temperature dependence of the luminescence intensities and life-times of each emission in $CdBr_2$:I. The broken lines, I_{UV} and I_G, show the temperature dependence of the UV- and the G-emission, respectively. The scale of the intensity is indicated on the right side ordinate. τ_{UV} and τ_G are the life-times of the UV- and the G-emission, respectively.

during which the luminescence intensity reduces to half as much as the initial one. More familiar life-time defined as the time interval during which the intensity reduces to 1/e is obtained by multiplying the present one by a factor, $\log_2 e = 1.443$. The life-time of the UV-emission, which is shown by solid circles, is 0.6 μs at LHeT and its temperature dependence is the same as that of the intensity. The decay curves of the Y-emission is composed of three components, which are shown in the figure by open circles (a), solid squares (b) and solid triangles (c). In the region of low temperature, the components (a), of 150 μs, and (c), of 2 μs, decrease gradually as the temperature rises. It was not possible to pull out the component (b) from the observed decay curves in any reliable manner at low temperatures.

In fig. 8 are shown the case of $CdBr_2$:I. In this case, the G-emission is observed in place of the Y-emission of $CdBr_2$. Overall behaviors of the temperature dependence are similar to those in $CdBr_2$. As shown by the dashed lines, the intensity of the UV-emission, which is dominant at low temperature, decreases around 60 K with the thermal activation energy ΔE = 0.07 eV and, instead, the G-emission becomes dominant at higher temperature. This emission is quenched above 180 K by thermal activation processes with ΔE = 0.31 eV. The life-time of the UV-emission is 0.3 μs and independent of temperature below 50 K. The life-time of the G-emission is 3 μs and independent of temperature from 70 K to 160 K. The rise in the life-time around 60 K may suggest the presence of another more longer component such as the component (a) of $CdBr_2$. It was not possible, however, in the lower temperature region to extract any components from the observed decay urves which behave in very complex manner.

With the hope to obtain more clear understanding of the relaxed excitonic states, the polarization of luminescence was measured. Results are shown in the following. In Fig. 9 are shown polarization characteristics of each emission band observed at LHeT and LNT. The lower part represents the emission spectra, just a simple reproduction of Fig. 6. Degree of polarization, P, is defined by

$$P = - \frac{I_{\parallel} - I_{\perp}}{I_{\parallel} + I_{\perp}} , \qquad (1)$$

where $I_{\parallel}$ and $I_{\perp}$ indicate the intensities of luminescence polarized parallel and perpendicular to the crystal c-axis, respevtively. Thus the upper points in this figure correspond to the luminescence highly polarized perpendicularly to the c-axis. Exciting light was projected along the c-axis on the cleaved surface of the crystal and the emis-

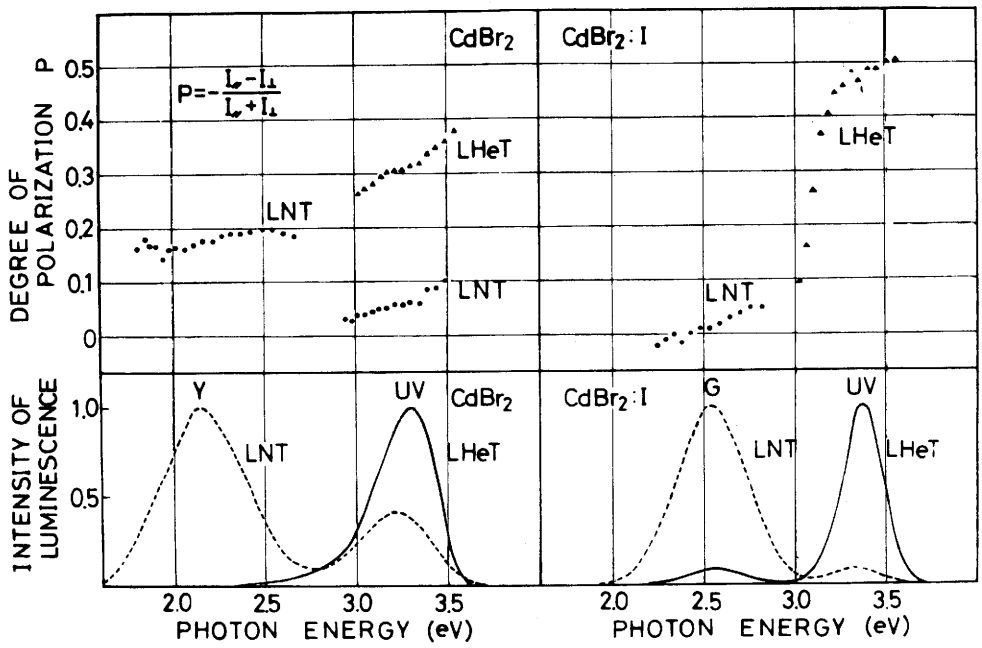

Fig. 9 Degee of polarization of each emission band in $CdBr_2$ and $CdBr_2$:I obtained at LHeT and LNT. The lower part represents the emission spectra, just a simple reproduction of Fig. 6. $I_{\parallel}$ and $I_{\perp}$ indicate the intensities of luminescence polarized parallel and perpendicular to the crystal c-axis, respectively. Excitation was made with nonpolarized light which was projected along the c-axis on the cleaved surface of the crystal. The emission was detected in the derection perpendicular to the crystal c-axis. The observed values of degree of polarization was corrected by using the calibration curve given in Fig. 3.

sion was detected in the direction perpendicular to it by using the calibrated apparatus shown in Fig. 3. In $CdBr_2$, the values of P of the Y-emission are about 0.2 at LNT and those of the UV-emission are 0.3 at LHeT and 0.05 at LNT. The values of P of the UV-emission are higher on the high energy side of the emission spectrum than on the low energy side. This suggests that the UV-emission is composed of two components,at least. In $CdBr_2$:I, the values of P of the G-emission are about zero at LNT and that of the UV-emission at LHeT is 0.5 on the high energy side of the emission band. On the low energy side, the value of P decreases rapidly, probably by the same reason as descrived above for the UV-emission in $CdBr_2$.

The values of P of the UV-emission depend not only on the emission

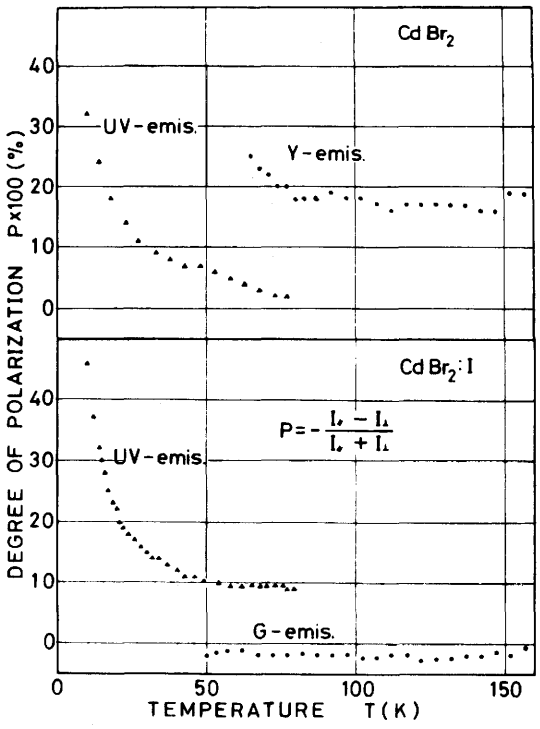

Fig. 10 The temperature dependence of degree of polarization of each emission in $CdBr_2$ and $CdBr_2$:I. Excitation was made with nonpolarized light projected along the *c*-axis on the cleaved surface of the crystal and the emission was detected in the direction perpendicular to the crystal *c*-axis. The observed values of degree of polariztion was corrected by using the caliblation curve in Fig. 3.

energy but also on temperature. In Fig. 10 are shown the temperature dependence of P for each emission. The values of P of the UV-emission decrease rapidly with raising temperature from 10 to 30 K in both cases of $CdBr_2$ and $CdBr_2$:I. This temperature dependence will be analyzed later by using a simple model with two close-lying levels, both of which are responsible for the UV-emission. The values of P of the Y- and G-emission are approximately constant in the region of high temperature. At low temperature, it was not possible to obtain reliable values of P for these emissions because of their weak intensities. Thus, we can tell nothing about the relaxed excitonic states responsible for these emissions from the present experimental results.

Polarization correlations were measured by using the excitation system shown in Fig. 4. Results are shown in Fig. 11. Here, the sign of P is chaged from that in Fig. 9 or 10. The directions of the crystal *c*-axis and the electric vectors of the exciting and emitted light are indicated in the figure. Solid curves are the reproduction of the absorption spectra in Fig. 5 and the ordinate scale of which is given on the right hand. Open and solid circles give the values of the degree of polarization for the excitation with the ultra-violet light polar-

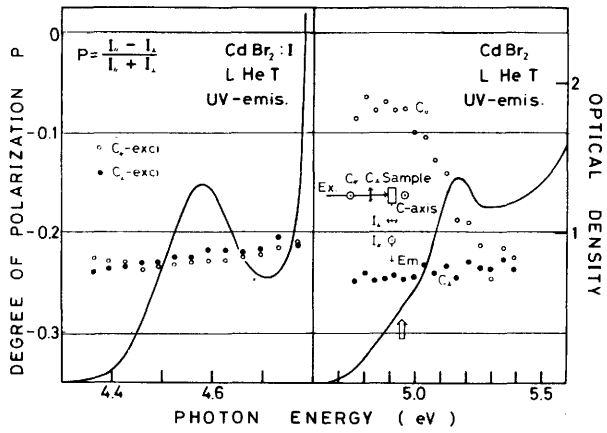

Fig. 11 Polarization correlation of the UV-emission observed at LHeT in $CdBr_2$ and $CdBr_2$:I. The directions of the crystal *c*-axis and the electric vectors of the exciting and emitted light are indicated in the figure. Open and solid circles give the observed values of the degree of polarization for the excitation with the ultra-violet light polarized along and perpendicularly to the *c*-axis, respectively. Note that the difinition of degree of polarization is changed sign from that in Fig. 9 and 10. The solid curves are the reproduction of the absorption spectra in Fig.5, the ordinate scale of which is given on the right hand.

ized along and perpendicularly to the *c*-axis, respectively. In $CdBr_2$:I, there is no correlation in the region of the localized excitonic absorption band. In $CdBr_2$, a remakable correlation was observed in the region of the 4.95 eV absorption shoulder, which is indicated in the figure by an arrow. The correlation diminishes as the excitation goes to the high energy regions. These results on the polarization correlation suggest that the excitonic states responsible for the 4.95 eV absorption in $CdBr_2$ are closely related with the RES responsible for the UV-emission and that the memory of the polarization in the exciting light will be lost through the relaxzation processes from the higher excitonic states to the RES. Details of these excitonic states are discussed in the next section.

4. Discussion

In the previous papers on the absorption and luminescence in $CdCl_2$-$CdBr_2$ and $CdCl_2$-$CdBr_2$:I mixed crystals[5,6,7], it has been reported that the concentration dependence of luminescence in the mixed crystals indicate the following facts. The constituent halogen ions of the solid solutions, Br^- and Cl^-, have important influences on the nature of the luminescence and several halogen ions should be associated with the RES in the cadmium halide crystals. Taking into consideration the possibility of self-trapping of holes or excitons in the 4*d* levels of the cadmium ions, the excited states of $[Cd^{2+}X_6^-]^{4-}$ -complex molecular ions have been considered as a model for the RES in $CdBr_2$ or $CdCl_2$. Here, we attempt to interpret the present experimental results on this supposition.

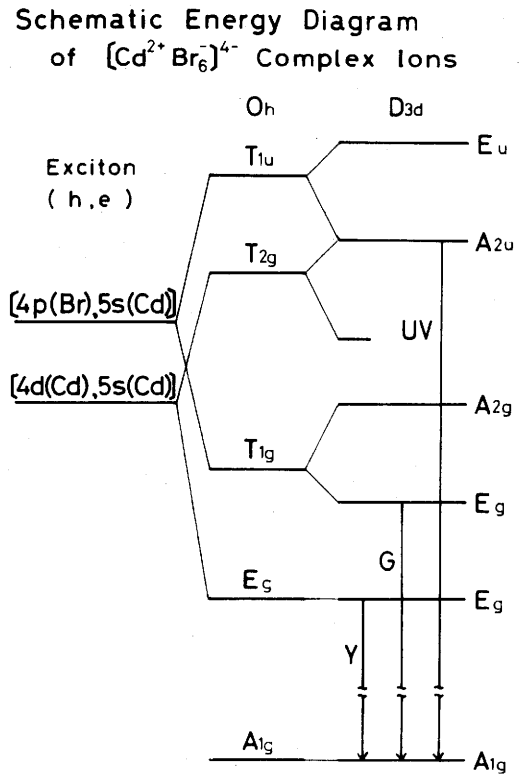

Fig. 12 Schematic energy diagram of $[Cd^{2+}Br_6^-]^{4-}$-complex molecular ion. In the left side are shown the possible excitonic states in arbitrary positions. In the middle column are shown the excited states of the complex molecular ion in O_h symmetry, which correspond to the relaxed states of the excitons shown in the left side. These states split into those shown in the right side in the case of D_{3d} symmetry. In this diagram under D_{3d} symmetry, the excited and ground levels are drawn so as the positions of the $A_{2u}(T_{1u})$, $E_g(T_{1g})$ and $E_g(E_g)$ levels relative to the $A_{1g}(A_{1g})$ ground level correspond to the energies of the UV-, G- and Y-emission bands, respectively. This energy diagram is drawn without taking the spin-orbit and electron-hole exchange interactions into consideration.

A schematic energy diagram of the complex molecular ions, $[Cd^{2+}X_6^-]^{4-}$, is shown in Fig. 12. In the left column of this figure are given possible configurations of excitons, the one composed of a $4p$ hole on the bromine ion and a $5s$ electron on the cadmium ion and the other composed of a $4d$ hole and a $5s$ electron on the cadmium ion. In the complex molecular ions, these excitonic states split into several states as shown in the middle column of the figure, where, for example, the T_{1u} state is an excitonic state with a hole on a nonbonding t_{1u} molecular orbital derived from the bromine $4p$ orbitals and an electron on an antibonding a_{1g} orbital derived mainly from the cadmium $5s$ orbitals. In the present case of D_{3d} symmetry, these states further split into the levels as shown in the right column of this figure. Before taking the important effects derived from the spin-orbit and exchange interactions into consideration, we have a trial of assignments of optical transitions associated with the UV-, Y_ and G-emission. The UV- emission, located at the highest energy, the life-time of which is relatively short and independent of temperature, may be connected with the parity allowed transition from the A_{2u} state to the ground A_{1g} state.

The transition from the E_u state to the A_{1g} state is not adequate for this emission as is explained later. The Y-emission, the lowest energy luminescence, with relatively long and temperature dependent life-times, may be associated with the parity forbidden transition from the lowest lying E_g state to the A_{1g} state. The forbiddenness may be partially broken by some odd parity perturbations, such as odd parity lattice vibrations. The G-emission in $CdBr_2$:I is regarded as an intrinsic one of $CdBr_2$ perturbed by the presence of iodine ions. The transition from the $E_g(T_{1g})$ state to A_{1g} state may be related with this emission, which is parity forbidden but partially allowed by some odd parity deformation caused bt the presence of neiboring iodine ions. The A_{2g} state is not favor for this emission because of the observed small values of degree of polarization. The odd parity perturbations associated with the Y- or G-emission would be those of the E_u mode, which mix both E_u and A_{2u} states to the E_g state to produce appropriate values of P according to the degree of mixing. Another odd parity mode, the A_{2u} mode, mix only the E_u state to the E_g state to bring about luminescence polarized perpendicularly to the c-axis perfectly. This is not the case of experimental results. It should be noted here that the above description is based on the energy diagram

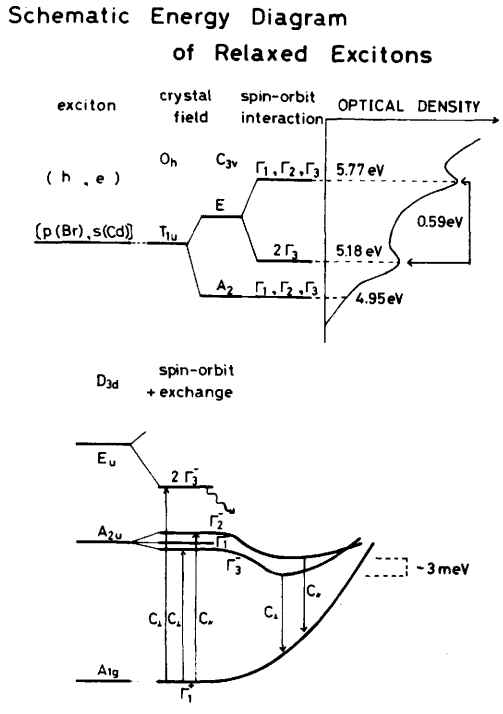

Fig. 13 Schematic energy diagrams of the excitonic and relaxed excitonic states in $CdBr_2$. The upper part shows the excitonic states related to the intrinsic absorption. The excitonic state associated with the transition in the interband edge region corresponds to the T_{1u} state in the bromine excitation model under O_h crystal field. Under the actual field of C_{3v} at the bromine ion site in $CdBr_2$, the T_{1u} state split into E and A_2. By introducing the spin-orbit interaction, it is possible to assign transitions associated with the observed absorption structures shown in the right side. The relaxed excited states corresponding to the above excitonic states are shown in the lower part. The E_u and A_{2u} states indicate those given in Fig.12. By introducing spin-orbit and exchange interactions, these states split into those shown in the middle column. Optical selection rules is indicated in the figure. $C_{\parallel}$ and $C_{\perp}$ correspond to optical transitions allowed with light polarized parallel and perpendicularly to the crystal c-axis, respectively.

of Fig. 12 which is drawn without taking the spin-orbit and exchange interactions into consideration. We can not make further discussions at present about the Y- and G-emission since there are no available data on the polarization characteristics at lower temperatures. Hereafter, we restrict our consideration to the UV-emission.

In Fig. 13 are shown schematic energy diagrams of the excitonic and the relaxed excitonic states in $CdBr_2$. In these diagrams, the spin-orbit and exchange interactions are taken account of to examine the observed polarization correlation in $CdBr_2$ shown in Fig. 11. The upper part shows the excitonic states related to the intrinsic absorption. In cadmium halide, it is believed that the top of the valence band consists mainly of the *p*-state in the halogen ion and the bottom of the conduction band mainly of the *s*-state in the cadmium ion. Thus, the exciton associated with the interband transition edge region may be composed of a *p*-like hole and a *s*-like electron. This excitonic state corresponds to the T_{1u} state in the O_h crystal field. By the C_{3v} trigonal field around the bromine ions, the excitonic state splits into the E and A_2 states. These states further split as shown in the figure by introducing the spin-orbit interaction; the E state into $\Gamma_1 + \Gamma_2 + \Gamma_3$ and $2\Gamma_3$, and the A_2 state becomes $\Gamma_1 + \Gamma_2 + \Gamma_3$. These three excitonic states may be connected with the observed absorption structures as is shown in the side of this figure.

In the relaxed excitonic states, excitonic states would be E_u and A_{2u} under the D_{3d} crystal field which is already shown in Fig. 12. By taking account of the spin-orbit and the electron-hole exchange interactions, these states split into several close-lying states as is shown in the lower part of Fig. 13. For example, the A_{2u} state split into the Γ_1^-, Γ_2^- and Γ_3^- states. Optical selection rules are shown in the figure, that is, the transition between the Γ_3^- and Γ_1^+ states is allowed for the light polarized perpendicularly to the crystal *c*-axis and the transition between the Γ_2^- and Γ_1^+ states is allowed for the light polarized parallel to the *c*-axis. The Γ_2^- and Γ_3^- states derived from the A_{2u} state are responsible both for the 4.95 eV absorption and the UV-emission as is depicted schematically in the figure. Thus, in the case of the excitation in the 4.95 eV absorption band, a remarkable polarization correlation would be observed in favor of the experimental results shown in Fig. 11. The Γ_2^- state must be located higher than the Γ_3^- state since the UV-emission following the excitation with the *c*-parallel light still polarize perpendicularly to the *c*-axis. The exchange splitting energy between the Γ_2^- and Γ_3^- state in the relaxed situations is about 3 meV which is estimated from the analysis of the

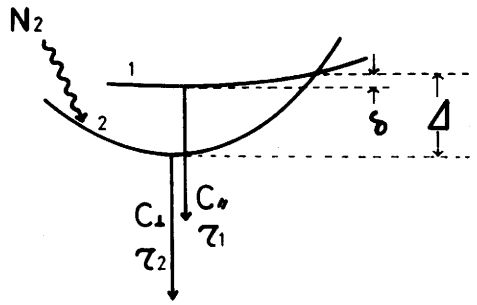

Fig. 14 Schematic one coodinate configurational scheme associated with the dynamical behavior of the UV-emission. Level 1 and 2 correspond to the $\Gamma_2^-(A_{2u})$ and $\Gamma_3^-(A_{2u})$ states in Fig. 13. N_2 is the excitation rate of the level 2. Δ and δ is the thermal activation energies for the nonradiative transitions between these levels.

temperature dependence of the polarization ratio of the UV-emission. On the other hand, the upper Γ_3^- state derived from the E_u state is responsible for the 5.18 eV absorption and is supposed not to contribute directly to any emission. Excitons created in this state by optical excitations may relax to the lowest Γ_3^- state and decay to the ground state accompanied with the UV-emission. In this case, the memory of polarization in the exciting light will be lost through the relaxation processes and so the correlation of polarization become small. The reason why the excitons may relax to the lowest Γ_3^- state, not to the Γ_2^- state, will be explained later.

The temperature dependence of polarization of the UV-emission can be explained by using a simple model with two close-lying levels which correspond to the Γ_2^- and Γ_3^- states in Fig. 13. In Fig. 14, the level 1 (the Γ_2^- state) is responsible for the emission polarized along the c-axis with the radiative life-time τ_1 and the level 2 (th Γ_3^- state) for that polarized perpendicularly to the c-axis with radiative life-time τ_2 . The thermal activation energies are taken as δ and Δ for the nonradiative transitions between these levels. Providing only the level 2 is populated by the optical excitation, the rate equations describing the dynamical behaviors of the relaxed excitons are represented as

$$\frac{dn_1}{dt} = -n_1 W_{12} \exp\left(-\frac{\delta}{\kappa T}\right) + n_2 W_{21} \exp\left(-\frac{\Delta}{\kappa T}\right) - \frac{n_1}{\tau_1} \qquad (2)$$

$$\frac{dn_2}{dt} = N_2 + n_1 W_{12} \exp\left(-\frac{\delta}{\kappa T}\right) - n_2 W_{21} \exp\left(-\frac{\Delta}{\kappa T}\right) - \frac{n_2}{\tau_2} \qquad (3)$$

where n_1 and n_2 are the populations of each level, N_2 the excitation rate of the level 2, W_{12} and W_{21} are the transition probabilities

from 1 to 2 and from 2 to 1, respectively, and κ the Boltzmann constant. In the case of the steady excitation, differentials of n_1 and n_2 vanish and the intensity ratio of $I_{//}$ to $I_{\perp}$ (the polarization ratio) is derived as

$$\frac{I_{//}}{I_{\perp}} = \frac{n_1/\tau_1}{n_2/\tau_2} = \frac{\tau_2 W_{21}\exp(-\Delta/\kappa T)}{\tau_1 W_{12}\exp(-\delta/\kappa T) + 1} \tag{4}$$

Assuming that the values of δ is much smaller than κT, the value of the polarization ratio is expressed as

$$\frac{I_{//}}{I_{\perp}} = A\exp(-\Delta/\kappa T) \tag{5}$$

where A is a constant independent of temperature.

In Fig. 15 are shown the dependence of the observed polarization ratio on the inverse of temperature. Open and solid circles are those obtained in $CdBr_2$ and in $CdBr_2$:I, respectively. It is obvious that the polarization ratios decrease exponentially with the inverse of temperature and tend to become unity at very high temperature. The straight lines are drawn according to the equation (5) by selecting appropreate values of Δ. Excellent agreement between the observed values and the ones calculated according to the equation (5) is obvious in this figure. The values of the activation energy, Δ, are 3.3 meV in $CdBr_2$ and 4.7 meV in $CdBr_2$:I. These values give approximately the exchange splitting energy between the levels, Γ_2^- and Γ_3^-. As is easily shown, the polarization ratio does not have a simple exponential dependence on $1/T$ if we assume the level 1, the Γ_2^- state, to be populated by the optical excitation. Thus, as described before, the excitons created in the $\Gamma_3^-(E_u)$ state by the optical excitation should

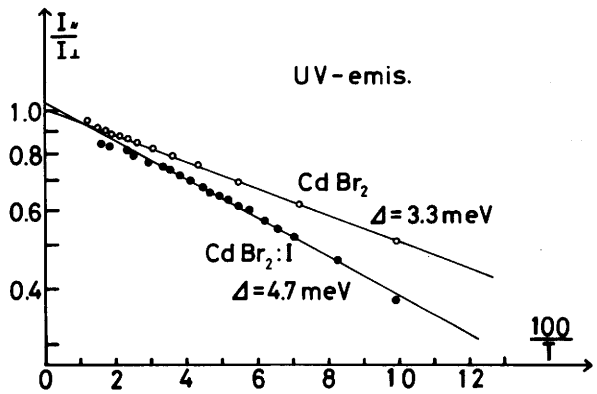

Fig. 15 The dependence of the polarization ratio on the inverse of temperature of the UV-emission in $CdBr_2$ and $CdBr_2$:I. Open and solid circles show the values obtained experimentally in $CdBr_2$ and $CdBr_2$:I, respectively. Straight lines are drawn by using the values of the activation energy Δ indicated in the figure.

not relax to the $\Gamma_2^-(A_{2u})$ state, but to the lowest lying $\Gamma_3^-(A_{2u})$ state.

5. Conclusion

The experimental results on the temperature dependence of the luminescence life-time and linear polarization in $CdBr_2$ and $CdBr_2$:I are well explained by assuming that the relaxed excitonic states in $CdBr_2$ are described by the excited states of the complex molecular ion consisting of a central cadmium and six neighboring bromine ions, $[Cd^{2+}Br_6^-]^{4-}$. In particular, polarization characteristics of the UV-emission is satisfactorily explained with this model by introducing the spin-orbit and electron-hole exchange interactions as well as the D_{3d} crystal field effect.

Acknowledgments

The authors wish to thank Professor H. Yagi and members of Experimental Institute for Low Temperature Physics, Fukui University, for supplying liquid nitrogen and liquid herium. We would like to thank Messrs. T. Yamada, K. Tachi, S. Tsuchida and K. Hirai for their technical and experimental assistance.

References

1) B. L. Evans: *Physics and Chemistry of Materials with Layered Structures, Vol. 4, Optical Properties of Layer Compounds in Optical and Electrical Properties* ed. P. A. Lee (D. Reidel Publishing Company, Dordrecht-Holland, 1976).
2) R. W. G. Wyckoff: *Crystal Structure* (John Wily and Sons, New York, 1963) 2nd ed., Vol. 1, p.270.
3) T. Kitamura, H. Nakagawa and H. Matsumoto: Memoirs Fac. Engng. Fukui Univ. **23** (1975) 57.
4) A. B. Lyskovich, S. K. Zherebetsy and G. M. Pentsak: Ukr. Fiz. Zh. **12** (1967) 800.
5) H. Nakagawa, K. Hayashi and H. Matsumoto: Memoirs Fac. Engng. Fukui Univ. **24** (1976) 211.
6) H. Nakagawa, K. Hayashi and H. Matsumoto: J. Phys. Soc. Japan **43** (1977) 1655.
7) K. Hayashi, H. Nakagawa and H. Matsumoto: Memoirs Fac. Engng. Fukui Univ. **25** (1977) 37.
8) M. R. Tubbs: Phys. Stat. Solidi (b) **49** (1972) 11.
9) S. Kondo and H. Matsumoto: Memoirs Fac. Engng. Fukui Univ. **25** (1977) 41.

10) H. Nakagawa, T. Abe and H. Matsumoto: J. Phys. Soc. Japan **40** (1976) 1363.
11) N. Nagasawa: J. Phys. Soc. Japan **27** (1969) 1535.
12) H. Matsumoto and H. Nakagawa: J. Luminescence **12/13** (1976) 403.